Research Article

Advances in Mechanical Engineering

Advances in Mechanical Engineering
2016, Vol. 8(7) 1–11
© The Author(s) 2016
DOI: 10.1177/1687814016657945
aime.sagepub.com
SAGE

Dynamic responses of space solar arrays considering joint clearance and structural flexibility

Yuanyuan Li[1], Zilu Wang[2], Cong Wang[1] and Wenhu Huang[1]

Abstract

This article numerically investigates the effects of revolute joint clearance and structural flexibility on the overall dynamic characteristics of a deployable solar array system. Considering torque spring, close cable loop configuration, and lock mechanism, a typical mechanism composed of a main body with a yoke and two panels is used as a demonstration case to study the effects of clearance and flexibility on the dynamic response of the deployable solar array system in the deployment and lock process. The normal contact force model and tangential friction model in clearance joint are established using Lankarani Nikravesh model and modified Coulomb friction model, respectively. The numerical simulation results reveal that the coupling of clearance and flexibility makes different effects on the dynamic characteristics of the deployable space solar arrays for different operation stages. Besides, the clearance and flexibility of a mechanical system play crucial roles in predicting accurately the dynamic response of the system, which is the foundation of mechanism design, precision analysis, and control system design.

Keywords

Deployable solar arrays, clearance joint, flexibility, dynamic responses, contact

Date received: 24 March 2016; accepted: 10 June 2016

Academic Editor: Mario L Ferrari

Introduction

Solar array, which provides necessary power for the whole system, is a vital component of the spacecraft widely used in space applications.[1] Deployable multiple-panel solar array system can be transformed from folded configuration during spacecraft launch and ascent to an expanded form with a larger volume when the spacecraft is turned into free flying orbit. The failure of the solar array deployment would be a disaster for a space mission. Therefore, it is very important to study the dynamic characteristics of the deployable space solar array system.

Dynamics of the deployable space structure with pinned joints can be divided into two parts: one is the flexible multibody dynamics, and the other is the clearance problem in joints.[2]

Up to now, the deployment of flexible solar array has been studied by many researchers. Wallrapp and Wiedemann[3] used the multibody program SIMPACK to simulate the deployment of a solar array three-dimensionally and to check the influence of the flexibility of the solar array on the solar generator motions. The comparison of the results shows that flexible bodies cause a slightly changed torque in the closed cable

[1]School of Astronautics, Harbin Institute of Technology, Harbin, P.R. China
[2]School of Aerospace Engineering, Tsinghua University, Beijing, P.R. China

Corresponding author:
Cong Wang, School of Astronautics, Harbin Institute of Technology, Harbin 150001, P.R. China.
Email: alanwang@hit.edu.cn

Creative Commons CC-BY: This article is distributed under the terms of the Creative Commons Attribution 3.0 License (http://www.creativecommons.org/licenses/by/3.0/) which permits any use, reproduction and distribution of the work without further permission provided the original work is attributed as specified on the SAGE and Open Access pages (https://us.sagepub.com/en-us/nam/open-access-at-sage).

Downloaded from ade.sagepub.com by guest on September 29, 2016

loops. Y Kojima et al.[4] simulated the ADEOS spacecraft attitude response due to the stick-slip effect and evaluated their mathematical model of spacecraft, which composed of a main rigid body and flexible appendages. The attitude stability of flexible spacecraft is discussed in this article. XS Ge and YZ Liu[5] derived the Euler's equations of forced vibration of two flexible solar arrays and discussed attitude stability of flexible spacecraft. E Gao et al.[6] presented the methodology on modeling and simulating the deployment and locking processes of flexible solar panels for a satellite and revealed that the deployment process of flexible solar panels impacted the attitude of satellite. These researches provide a significant foundation for studying the dynamic characteristics of deployable flexible solar array system during deployment.

On the other hand, many scholars have done a lot of researches on the deployable mechanisms with clearance joints. Clearance in joints is the necessary condition to ensure the deployable structure deploy smoothly and reliably. The emergence of the contact, collision, friction, and impact in clearance joints will cause severe vibration and nonlinear dynamic responses of the deployable space structures.[7,8] The clearance joints in multibody system cause significant effects on the deployment kinematics performance and dynamic performance. Flores[9] proposed a computational methodology to quantify the influence of the clearance size, friction coefficient, and number of clearance joints on the dynamic response of planar rigid multibody systems, which provided references for the dynamic analysis of multibody mechanical systems with multiple clearance joints. Besides, Flores et al.[10,11] showed that the existence of dry friction at joint clearances caused high peaks on the kinematic and dynamic responses when compared to those obtained with lubricated model. The performance of the lubricated joint is closer to that of an ideal joint. Muvengei et al.[12] numerically investigated the parametric effects of differently located frictionless revolute clearance joints on the overall dynamic characteristics of a multibody system, and the results showed that location of the clearance revolute joint, the clearance size, and the operating speed of a mechanical system play crucial roles in predicting accurately the dynamic responses of the system. Bai and colleagues[13,14] quantitatively investigated the dynamic responses of a typical multibody system with revolute clearance joints and investigated effects of clearance on dynamic responses of rigid dual-axis positioning mechanism of a satellite antenna. These studies and investigations revealed dynamic characteristics of mechanisms with clearance joints and provided basic modeling and analysis methods for some typical multibody systems.

However, researches on the effects of coupling of clearance and flexibility on the dynamics of a deployable mechanism, such as space solar arrays system, are insufficient for predicting the in-orbit performance of developable space mechanisms with clearance joints. J Li et al.[15] revealed that evidently nonlinear dynamic characteristics existed in the multibody deployable mechanism and investigated the effects of clearance, damping, friction, gravity, and flexibility on dynamic performance of multibody system. In addition, computational methodologies are presented for modeling and analysis of flexible planar multibody systems with clearance and lubricated revolute joints.[16,17] Zheng and Zhou[18] and Khemili and Romdhane[19] conducted the dynamic modeling of rigid-flexible coupling slider-crank mechanism with clearance based on the analysis/design software ADAMS. However, the coupling effects of joint clearance and structural flexibility on the dynamics of deployable space solar arrays is a complex nonlinear issue. Different from general closed multibody system, the deployable space solar arrays, as open multibody system, have their own dynamic phenomena, which is influenced by the particular close cable loop (CCL) configurations and lock mechanisms. The dynamic modeling of multibody solar array system with a full understanding of coupling between clearance and flexibility is an important foundation for simulation, design, analysis, optimization, and control of the mechanisms and manipulators.

Thus, this article establishes the dynamics model of solar array system with clearances, which consists of a main body, a flexible yoke and two flexible panels connected with clearance joints, torque springs, CCLs, and lock mechanisms. Then, the contact force model and friction effect model in the clearance are established. Finally, the effects of coupling of clearance and flexibility on the dynamic characteristics of the deployable space solar arrays are investigated.

Dynamic representation of solar array system with clearance joints

Structure of spacecraft system

Solar array system is the critical appendages of spacecraft. The spacecraft system adopted in this article is shown in Figure 1, which consists of a main body, a yoke, and two solar panels connected by revolute joints. The preloaded torsion springs located at each revolute joint provide the energy to deploy the arrays. The CCL configurations are applied as synchronous deployment control mechanism of appendages composed by a yoke and two solar panels. Besides, lock mechanisms located at revolute joints play a role in locking the arrays in the proper position.

Torque spring mechanism. The preloaded torque spring drives the array deployment in a preset speed. The dive

Downloaded from ade.sagepub.com by guest on September 29, 2016

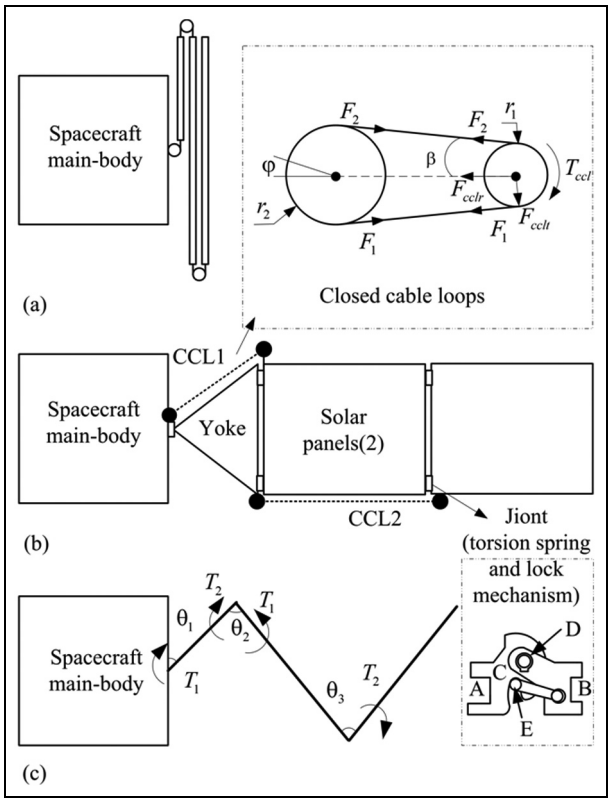

Figure 1. The structure of solar array system: (a) in folded condition, (b) the CCL connection diagram, and (c) the cable torque analysis model.

torque T^i_{dive} on the ith ($i = 1, 2, 3$) joint can be represented as

$$T^i_{dive} = K(\theta_{pre} - \theta) \tag{1}$$

where K is the torsional stiffness of torsion spring; θ_{pre} and θ are the preload angle and practical angle of the ith joint, respectively.

CCL configurations. CCL configurations as shown in Figure 1(b) are applied to achieve synchronous deployment of solar arrays. Folded arrays are released in orbit under the control of the flexible CCL configuration by synchronizing the deployment angles during the deployment. The CCL mechanism comprises synchronous wheels and pre-tensioned close-loop cables. Figure 1 illustrates the forces and torques of a typical CCL. The tight-side tension F_1 and slack-side tension F_2 can be expressed by

$$\begin{cases} F_1 = F_0 + (d - d_0)K_{ccl} + \varphi r_1 K_{ccl} \; F_1 \geq 0 \\ F_2 = F_0 + (d - d_0)K_{ccl} - \varphi r_1 K_{ccl} \; F_2 \geq 0 \end{cases} \tag{2}$$

where K_{ccl} is the equivalent elastic stiffness; F_0 is the preload in the belt; d_0 is the initial distance between two wheels; d is the real distance under tension; φ is the relative rotation angle of two wheels; r_1 and r_2 are the radius of the wheels.

When the two arrays are not synchronous, the tight-side tension F_1 and slack-side tension F_2 will provide a torque T_{ccl}. Then

$$\begin{cases} F_{cclr} = (F_1 + F_2)\cos\beta \\ F_{cclt} = (F_1 + F_2)\sin\beta \\ L_{ccl} = (F_1 - F_2)r_1 = 2\varphi r_1^2 K_{ccl} \end{cases} \tag{3}$$

where β is the angle between the center line of two wheels and the belt.

CCL configurations synchronize the deployment angles of each panel by applying a passive control torque proportional to the angle difference. Therefore, the torques of passive control (Figure 1(c)) can be regarded as

$$\begin{cases} T_1 = n\varphi r_1^2 K_{ccl} = K_1(2\theta_1 - \theta_2) \\ T_2 = \varphi r_1^2 K_{ccl} = K_2(\theta_2 - \theta_3) \end{cases} \tag{4}$$

where T_1 and T_2 are the equivalent synchronous torques generated by the CCL; K_1 and K_2 are the equivalent torsional stiffness of wheels; n is the ratio of the wheels; θ_1, θ_2, and θ_3 are the deployment angles.

Lock mechanism. A schematic diagram of lock mechanism is shown in Figure 1. The joint connects two bodies A and B separately; the two bodies rotate relatively round the joint D. The pin E can move on the surface of C in the deployment process. The pine slide into the groove until the deployment angle θ_i reaches the preset lock angle. Thus, the lock mechanism is activated and the two bodies are locked. In addition, the lock angle between spacecraft and yoke is 0.5π, and the angle between other panels is π.

A STEP function and a BISTOP function are introduced to present the equivalent moment T_{lock} in the lock mechanism as

$$\begin{cases} \text{when the mechanism is unlocked} \\ T_{lock} = 0 \\ \\ \text{when the mechanism is locked} \\ T_{lock} = \text{STEP}(\theta_i, x_1, 0, x_2, 1) \times \\ \text{BISTOP}(\theta_i, \dot{\theta}_i, x_3, x_4, K_{bs}, e, C, d) \end{cases} \tag{5}$$

$$\text{STEP}(\theta_i, x_1, h_1, x_2, h_2) = \begin{cases} \text{if } \theta_i < x_1\text{: } 0 \\ \text{if } x_1 \leq \theta_i \leq x_2 : \\ h_1 + (h_2 - h_1)\left(\dfrac{\theta_i - x_1}{x_2 - x_1}\right)^2 \left(3 - 2 \times \dfrac{\theta_i - x_1}{x_2 - x_1}\right) \\ \text{if } \theta_i > x_2\text{: } 1 \end{cases} \tag{6}$$

Downloaded from ade.sagepub.com by guest on September 29, 2016

$$\mathrm{BISTOP}(\theta_i, \dot{\theta}_i, x_3, x_4, K_{bs}, e, C_{\max}, d) =$$
$$\begin{cases} \text{if } \theta_i < x_3: \\ \mathrm{Max}(K_{bs}(x_3 - \theta_i)^e - \dot{\theta}_i step(\theta_i, x_3 - d, C_{\max}, x_3, 0), 0) \\ \text{if } \theta_i > x_4: \\ \mathrm{Min}(-K_{bs}(\theta_i - x_4)^e - \dot{\theta}_i step(\theta_i, x_4, 0, x_4 - d, C_{\max}), 0) \end{cases} \tag{7}$$

where θ_i is the angle at the ith joint; $\dot{\theta}_i$ is the rotation velocity of the ith lock mechanism; K_{bs} and $C_{\max}$ are the stiffness and damping coefficients of the corresponding lock mechanism, respectively; e is an exponent; and d is the distance depth. The STEP function approximates the Heaviside step function with a cubic polynomial increases from h_1 to h_2. The BISTOP function allows free motion between x_3 and x_4 at which point the contact function begins to push the joint back toward the expect center angle.

Clearance revolute joint model

Multibody system with joint clearance dynamics model. The intermittent collision and friction exit inside the clearance joints of multibody system. The relative motion states of pin and sleeve are divided into the free movement and contact deformation phases. The dynamics equation of multibody system is calculated using the Lagrange multiplier method. In the free movement phase, the system dynamic equation can be described by

$$\begin{aligned} &\mathbf{M}\mathbf{q} + \mathbf{C}\dot{\mathbf{q}} + \mathbf{K}\mathbf{q} + \mathbf{\Phi}_{\mathbf{q}}^{\mathbf{T}}\boldsymbol{\lambda} = \mathbf{f} \\ &\mathbf{\Phi}(\mathbf{q}, t) = 0 \end{aligned} \tag{8}$$

where $\mathbf{q}$ and $\ddot{\mathbf{q}}$ are the generalized coordinate column matrix and acceleration vectors matrix, respectively. $\mathbf{M}$, $\mathbf{C}$, and $\mathbf{K}$ are the generalized mass matrix, damping matrix, and stiffness matrix of the multibody system, respectively. $\mathbf{\Phi}_q$ is the Jacobi matrix of constraint equation. $\boldsymbol{\lambda}$ is the Lagrange multiplier column matrix, and $\mathbf{f}$ is the generalized force matrix.

In the contact deformation phase, the contact forces occur in the clearance joints between two colliding bodies. Thus, the system dynamic equation can be obtained by

$$\begin{aligned} &\mathbf{M}\ddot{\mathbf{q}} + \mathbf{C}\dot{\mathbf{q}} + \mathbf{K}\mathbf{q} + \mathbf{\Phi}_{\mathbf{q}}^{\mathbf{T}}\boldsymbol{\lambda} = \mathbf{f} + \mathbf{F}_c \\ &\mathbf{\Phi}(\mathbf{q}, t) = 0 \end{aligned} \tag{9}$$

where $\mathbf{F}_c$ is the contact force relative to $\mathbf{q}$.

As shown in Figure 2, the types of contact force in clearance joints contain normal contact force F_n, tangential friction force F_f, and resistance moment M.

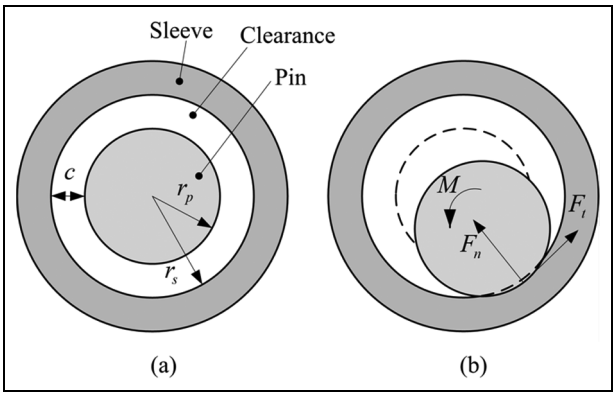

Figure 2. Clearance joint model: (a) free movement and (b) contact deformation.

Normal contact force model. Force normal to the direction of contact appears when the pin makes contact with the sleeve. Hertz contact law reveals the contact force as a nonlinear function related to penetration depth. Unfortunately, Hertz contact law cannot be used in compression and restitution phase of contact as the law ignores the energy dissipation during the impact process. Lankarani and Nikravesh[20] modified the Hertz contact force model considering energy dissipation during the impact process by introducing a hysteresis damping function. The Lankarani Nikravesh model including the energy dissipation in the form of internal damping has been adopted by a lot of researchers and has been proved effective by comparing the theoretical results and the related experimental ones. Thus to accurately investigate the dynamic performance of multibody system with revolute clearance joint and calculate the contact force in clearance joint, in this article, the nonlinear contact force model proposed by Lankarani and Nikravesh is applied for the contact force model between the pin and sleeve. It can be expressed as

$$F_n = K\delta^n + D\dot{\delta} \tag{10}$$

where F_n is the normal contact force, exponent $n = 1.5$ for metallic surfaces, δ is the indentation depth of the contacting bodies, and $\dot{\delta}$ is the relative impact velocity. The equivalent stiffness K can be calculated according to the material property parameters and geometrical shape of the contact surfaces, which is obtained as

$$\begin{aligned} K &= \frac{4}{3\pi(\sigma_s + \sigma_p)}\left[\frac{r_s r_p}{r_s - r_p}\right]^{\frac{1}{2}} \\ \sigma_k &= \frac{1 - u_k^2}{\pi E_k}(k = s, p) \end{aligned} \tag{11}$$

where r_s and r_p are the radii of the pin and sleeve, respectively. E_k and u_k are Young's modulus and Poisson's ratio associated with each sphere, and D is the hysteresis coefficient given as

Downloaded from ade.sagepub.com by guest on September 29, 2016

Table 1. Geometrical and physical parameters of the solar deployment system.

	Length (mm)	Width (mm)	Thickness (mm)	Mass (kg)	Inertia I_{xx} (kg mm^2)	Inertia I_{yy} (kg mm^2)	Inertia I_{zz} (kg mm^2)
Main body	400	400	400	175.36	4.676×10^6	4.676×10^6	4.676×10^6
Yoke	150	150	5	0.0335	0.0938×10^6	0.1587×10^6	0.0651×10^6
Panel 1(2)	300	150	2	0.2466	0.4625×10^6	2.312×10^6	1.850×10^6

$$D = \frac{3K(1-C_e^2)\delta^n}{4\dot{\delta}^{(-)}} \tag{12}$$

where $\dot{\delta}^{(-)}$ is the initial impact velocity and C_e is the coefficient of restitution. Therefore, the final normal contact force can be expressed as

$$F_n = K\delta^n\left[1 + \frac{3(1-C_e^2)\dot{\delta}}{4\dot{\delta}^{(-)}}\right] \tag{13}$$

Tangential friction force model. In addition to the normal contact force, the clearance joint forces may be enhanced by considering the effect of friction. Tangential motion between two contact bodies contains relative slip status and viscous status. In this article, a modified Coulomb friction model with better numerical features is applied to describe the dry friction response between the pin and sleeve. The direction is tangent to the contact surface. It can be evaluated as

$$F_f = -\mu(v_t)F_n \tag{14}$$

where friction coefficient $\mu(v_t)$ is a function of tangential sliding velocity and it can be expressed as

$$\mu(v_t) = \begin{cases} \text{if } |v| > v_d : -\mu_d \text{ sign}(v) \\ \text{if } v_s \le |v| \le v_d : -\text{STEP}(|v|, v_d, \mu_d, v_s, \mu_s)\text{sign}(v) \\ \text{if } |v| < v_s : \text{STEP}(v, -v_s, \mu_s, v_s, -\mu_s) \end{cases} \tag{15}$$

where v_t is relative sliding velocity of pin and sleeve at the collision point. μ_d and μ_s are dynamic friction coefficient and static friction coefficient, respectively. v_d and v_s are critical velocity of maximum dynamic friction and static friction, respectively.

Numerical simulation model of deployable solar array system

A deployable solar array system with clearance is modeled to analyze the dynamic responses of the solar array system during initial operation stage, deployment stage, and pre- and post-system lock stage, which is shown in Figure 3. The physical parameters of main body, yoke, and panels are shown in Table 1. In this article, the material of yoke and panels is aluminum, its density is 2.74×10^{-6} kg/mm^3, elastic modulus is 7.17×10^4N/mm^2, and Poisson's ratio is 0.33. The flexible body models of yoke and panels are established by finite element method. The first 3 typical frequencies of panel are 0.45, 1.79, and 3.09 Hz, and the corresponding frequencies of yoke are 2.72, 3.26, and 5.07 Hz. Finite element model is set up with shell element, mainly using QUAD4 elements, whose side length is approximately 7.5 mm. The typical eigenfrequencies and eigenmodes of the yoke and panel are shown in Figures 4 and 5. A damping ratio of 1% has been considered. The geometrical and physical parameters of revolute joints are shown in Table 2, where clearance $c = r_s - r_p = 0.1$ mm. For the ideal joints, $r_s = r_p = 4$ mm. The model has three driven torsion springs (torsion spring 1, torsion spring 2, and torsion spring 3) located at joint 1, joint 2, and joint 3, respectively. Parameters of torsion springs are shown in Table 3. In the clearance joint, equations (3)–(5) are applied in the numerical simulations of the deployable solar array system; the contact parameters are set as shown in Table 4. Stiction transition velocity and friction transition velocity used in the simulation, respectively, are 1 and 10 mm/s. During the simulation, the integration tolerance is 0.001 and the step size is 0.0001 s. Here, Gear stiff integrator is selected as integration method and SI1 is selected as integrator formulation.

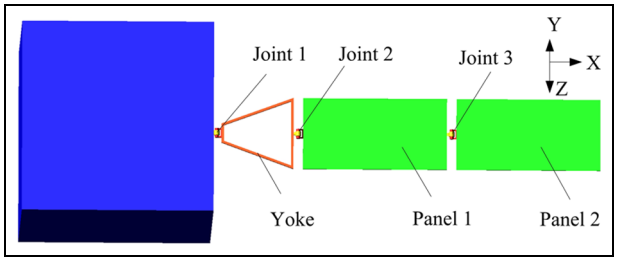

Figure 3. Simulation model of solar array system.

Results and discussion

Dynamic responses of deployable rigid solar array system with ideal joints

The folded solar array system is released driven by torsion springs and deployed under the control of CCL

Downloaded from ade.sagepub.com by guest on September 29, 2016

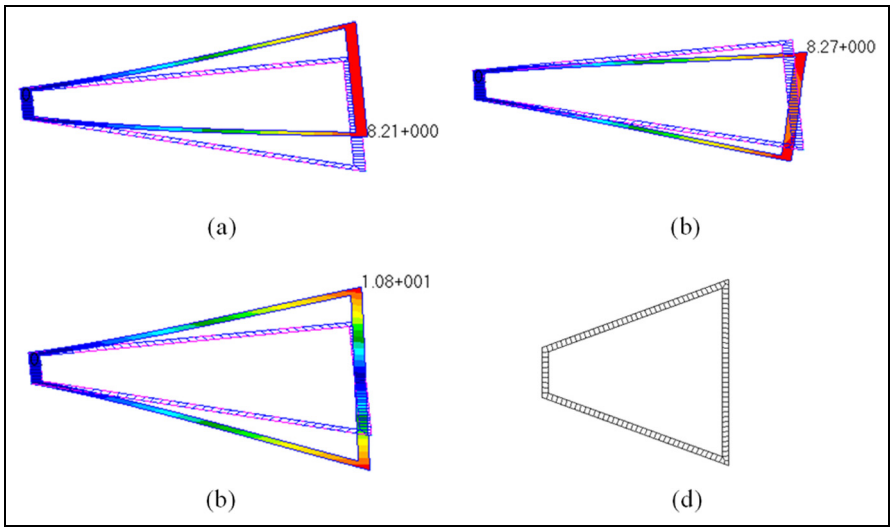

Figure 4. Flexible yoke: three typical eigenfrequencies and eigenmodes: (a) first mode and natural frequency: 2.72 Hz, (b) second mode and natural frequency: 3.26 Hz, (c) second mode and natural frequency: 5.07 Hz, and (d) meshing elements of yoke.

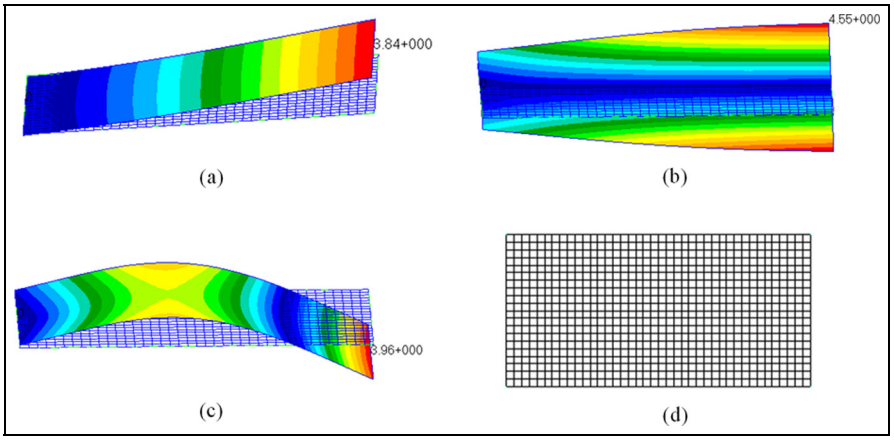

Figure 5. Flexible panel: three typical eigenfrequencies and eigenmodes: (a) first mode and natural frequency: 0.45 Hz, (b) second mode and natural frequency: 1.79 Hz, (c) second mode and natural frequency: 3.09 Hz, and (d) meshing elements of panel.

Table 2. Geometrical and physical parameters of revolute joints.

	Radius (mm)	Young's modulus (N/mm^2)	Poisson's ratio	Material	Mass (kg)
Pin	$r_p = 4$	2.7×10^5	0.29	Steel	8.8×10^{-3}
Sleeve	$r_s = 4.1$	1.06×10^5	0.32	Brass	5.9×10^{-3}

mechanism. Finally, the whole system is locked at the expected deployment position by the lock mechanism. The dynamic response of deployment of rigid solar array system with ideal joints is calculated, as shown in Figure 6. The measurement objects (yoke, panel 1, and panel 2) are shown in Figure 3. Figure 6 illustrates that speed fluctuation happens in the deployment process due to the synchronous adjustment torques provided by CCL mechanism. Furthermore, a sudden change in the angular accelerations occurs at the end of deployment due to the lock torques provided by lock mechanism. After locked, the system can quickly achieve stability through a short time little jitter.

Effects of clearance

The deployment of the rigid solar array system with three 0.1-mm clearance joints is simulated to study the effect of clearance joints on dynamic performance of the structure. Taking results of yoke as an example,

Downloaded from ade.sagepub.com by guest on September 29, 2016

Table 3. Parameters of torsion springs.

	Torsional stiffness (N mm/°)	Preloaded angle (°)
Torsion spring 1	0.3	210
Torsion spring 2	0.1	545
Torsion spring 3	0.1	300

Table 4. Contact parameters.

Restitution coefficient, C_e	0.95
Contact stiffness, K (N/mm$^{3/2}$)	1.3×10^6
Dynamic friction coefficient, μ_d	0.15
Static friction coefficient, μ_s	0.2

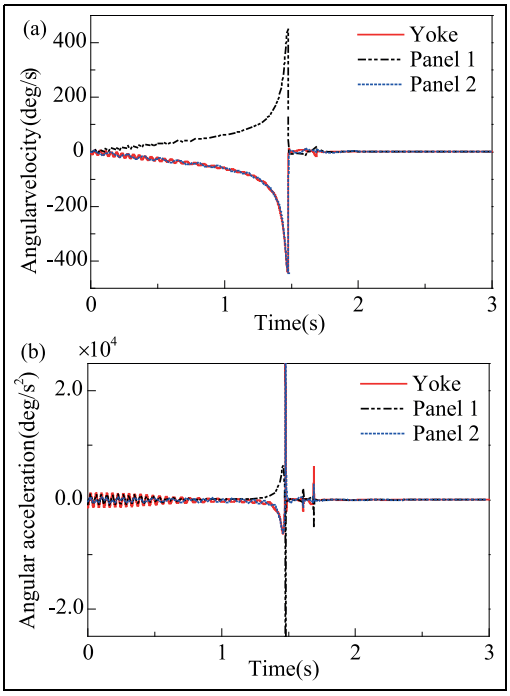

Figure 6. Dynamic responses of rigid solar array system with ideal joints: (a) angular velocity and (b) angular acceleration.

Figure 7 shows the angular velocity responses of rigid solar array system considering joint clearance. Figure 7(a) shows that the solar array system with clearance joints needs more time to achieve the deployment to the expect lock position influenced by the tangential friction force. Moreover, the speed fluctuation amplitude of the system with clearance reduces in the deployment process. Because the clearances can change the relative position between the pin and the sleeve, that decrease the deployment asynchrony angle in proportion to the synchronous adjustment torques provided by CCL mechanism according to equation (4), as shown in Figure 8.

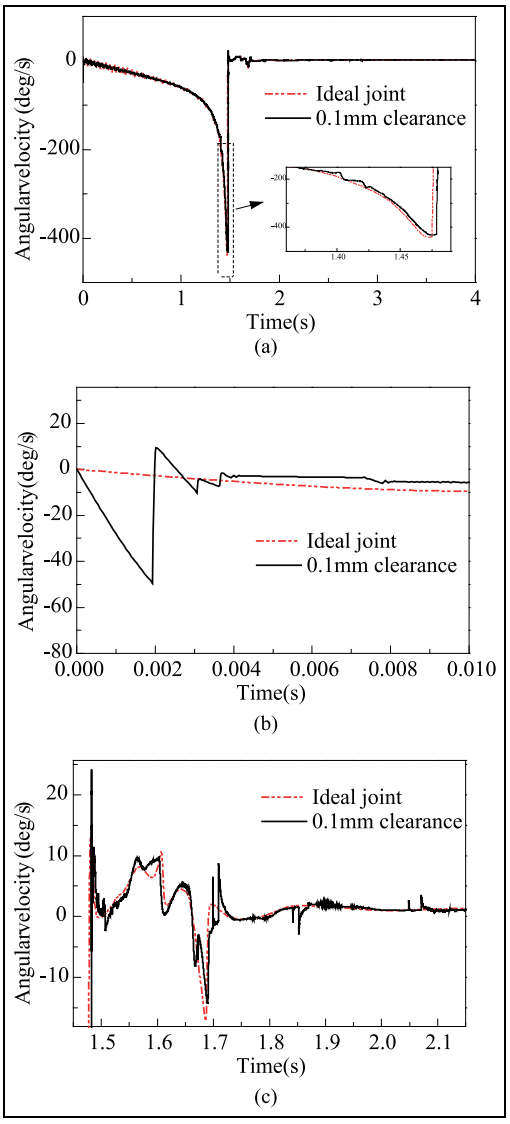

Figure 7. Angular velocity responses of rigid solar array system with 0.1-mm joint clearance: (a) the whole stages, (b) initial stage and (c) post-lock stage.

Furthermore, Figure 7(b) shows that clearances lead to severe impacts between pins and sleeves at the beginning of system operation. Besides, Figure 7(c) shows that the system with clearance needs more time to achieve stability and shake violently after locked because the contact force and lock force coupling provides a serious of discrete instantaneous impact force on the joint with clearance. Figure 9 shows the effect of clearance on solar array system lock torque at joint 1. Due to the joint clearance, pins and sleeves impact at the beginning of the system motion and keep on contact and impact in the later period after locked. The clearance in the joints influences the positioning accuracy, movement stability, and reliability of the mechanism system.

Downloaded from ade.sagepub.com by guest on September 29, 2016

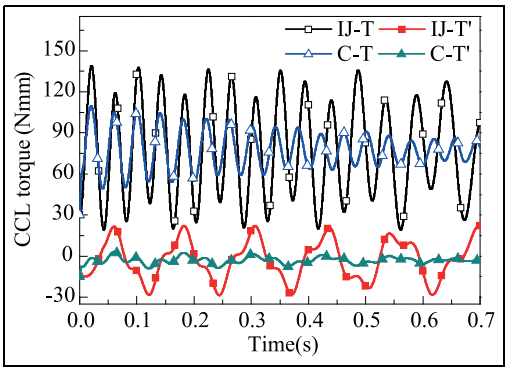

Figure 8. Synchronous adjustment torques provided by CCL1 mechanism. IJ-T: the torque close to the main body for system with ideal joint; IJ-T′: the torque far from the main body for system with ideal joint; C-T: the torque close to the main body for system with clearance; C-T′: the torque far from the main body for system with clearance.

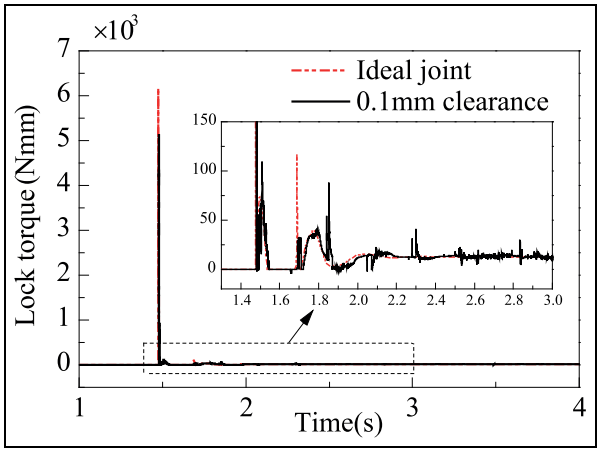

Figure 9. The lock torque of rigid solar array system with 0.1-mm joint clearance.

Effects of flexibility

Deployment of the flexible solar array system with ideal joints is simulated to study the effect of flexibility on the dynamic performance of solar array system. Compared with rigid bodies, elasticity deformations of flexible yoke and panels coupled to the rigid motion have a significant effect on the dynamic response of deployable solar arrays. The angular velocities and angular accelerations of flexible bodies shown in Figure 10 are markedly different with the results of rigid bodies shown in Figure 6. The vibrations of flexible bodies are more evident at two phases: the beginning of operation and after locked. At the moment of deployment startup, the sudden driving force causes the vibration of the flexible bodies; flexible bodies keep vibration for a period after locked.

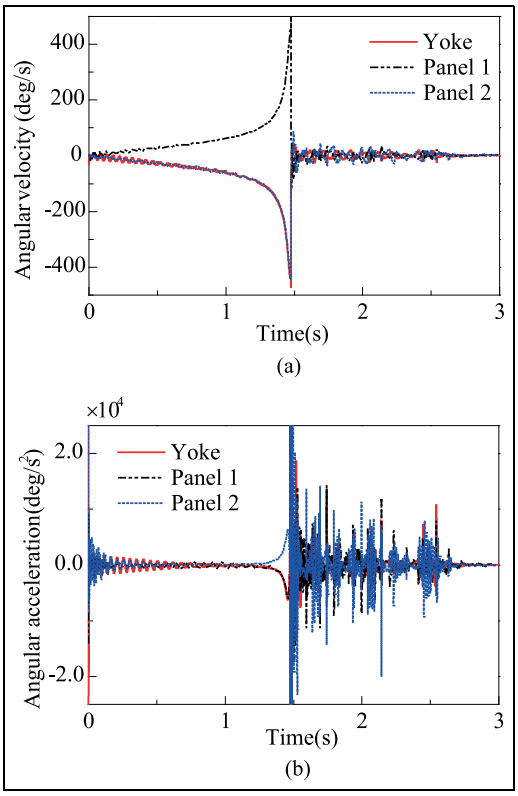

Figure 10. Dynamic responses of flexible solar array system with ideal joints: (a) angular velocity and (b) angular acceleration.

Effects of clearance and flexibility

Taking results of panel 2 as an example, Figure 11 shows the effect of clearance and flexibility on the angular velocity responses flexible solar array system. Compared with the rigid body, the flexible body has speed fluctuation caused by the synchronous adjustment torques and vibration caused by its own elastic deformation in deployment, as shown in Figure 11(b). Moreover, the clearances decrease vibration of the flexible body in most of deployment stage because the clearance can be seen as the equivalent spring-damping model calculated using equations (10)–(12). It means that flexible bodies with clearances can be seen as they with spring-dampers, which can control the system vibration compared to the ideal joints. Furthermore, solar array system has the larger vibration amplitude and the longer vibration time under the coupling effect between elastic vibration and impact in clearance joint before and after the lock time, as shown in Figure 11(b) and (c). Figure 12 shows the contact force at joint 3 in four cases: rigid bodies with ideal joints, flexible bodies with ideal joints, rigid bodies with clearances, and flexible bodies with clearances. For the cases of flexible yoke and panels, the maximum values of impact are highly reduced; the elastic yoke and panels act as a suspension system for the mechanism. However,

Downloaded from ade.sagepub.com by guest on September 29, 2016

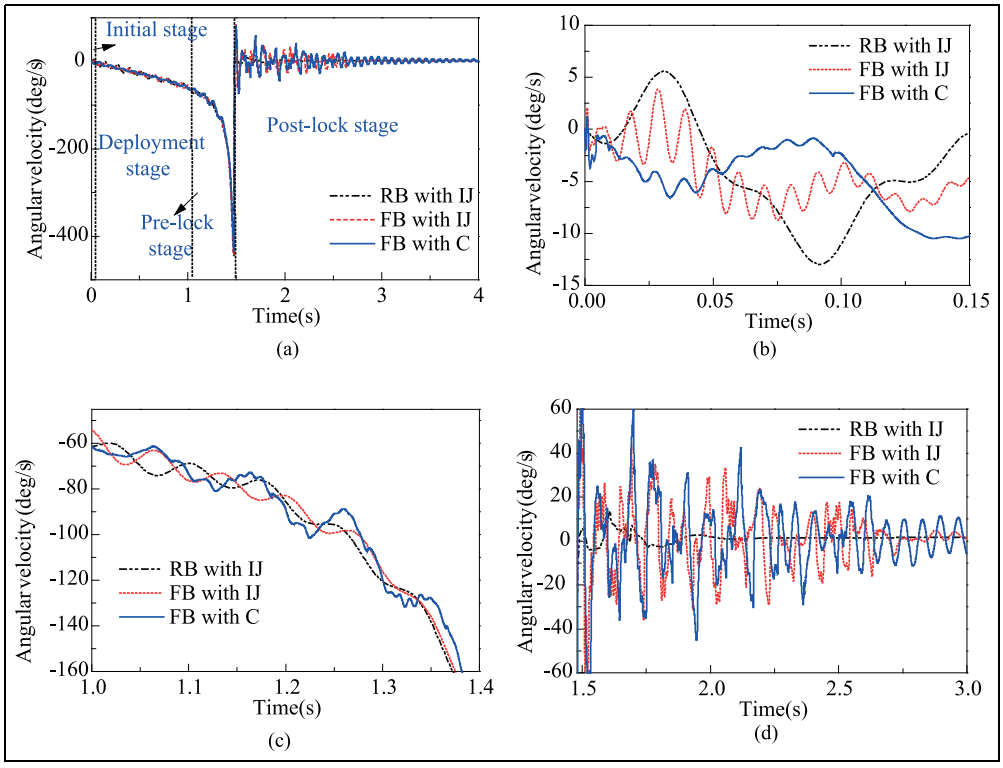

Figure 11. Angular velocity responses of flexible solar array system with 0.1-mm joint clearance. RB with IJ: rigid bodies with ideal joints; FB with IJ: flexible bodies with ideal joints; FB with C: flexible bodies with clearances: (a) the whole stages, (b) initial stage, (c) pre-lock stage and (d) post-lock stage.

obviously, flexible bodies with clearances have a serious of discrete instantaneous contact force at the post-lock stage because solar arrays as large flexible structures will remain excited for a long time after deployment. The structural vibration causes oscillation of the whole system and intensifies collisions at clearances between pins and sleeves. Compared with the contact force of rigid body with clearance, the clearance contact force of flexible body is denser and influenced by the coupling of elastic vibration and impact, especially pre- and post-lock time.

The relative position track between the center of pin and sleeve at the clearance joint 1 is shown in Figure 13, and the impact frequency becomes obviously higher and impact trace is more disordered. Figure 14(a) and (b) shows time histories of the displacement and velocity in y direction of the mass center of spacecraft main body in four cases, respectively. The unbalanced driving moment, lock torque, contact, impact, friction force, and so on generated by deployment of solar arrays may disturb spacecraft attitude. The results indicate that the clearance and flexibility of the solar arrays system have obvious effects on the dynamic characters of space main body. Clearance and flexibility change the lock position accuracy and deployment time. Rigid body with ideal joints has more obvious velocity perturbation

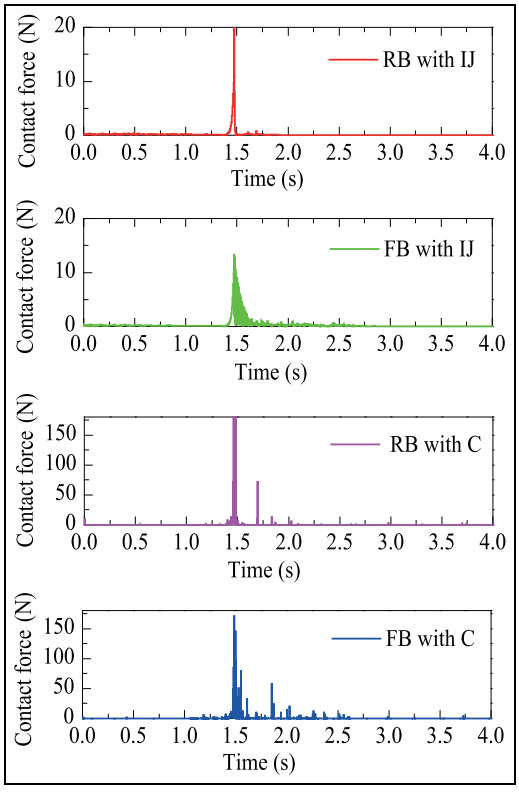

Figure 12. Contact force at joint 3.

Downloaded from ade.sagepub.com by guest on September 29, 2016

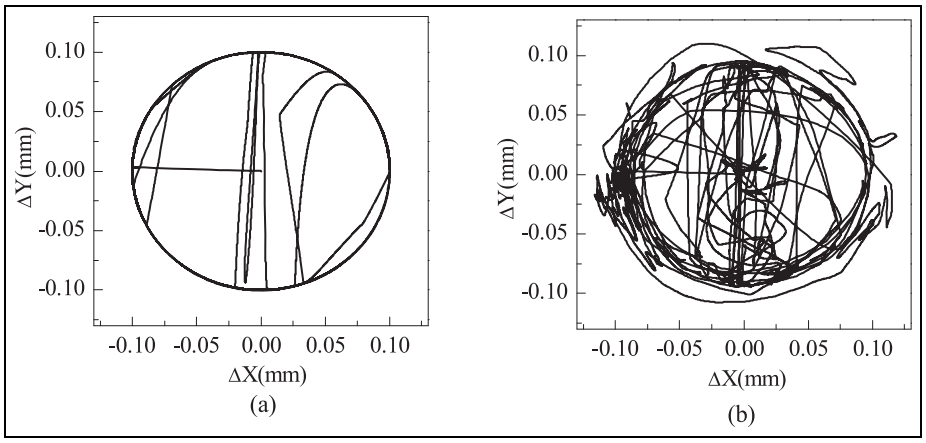

Figure 13. Impact track of the clearance joint: (a) impact track of rigid bodies and (b) impact track of flexible bodies.

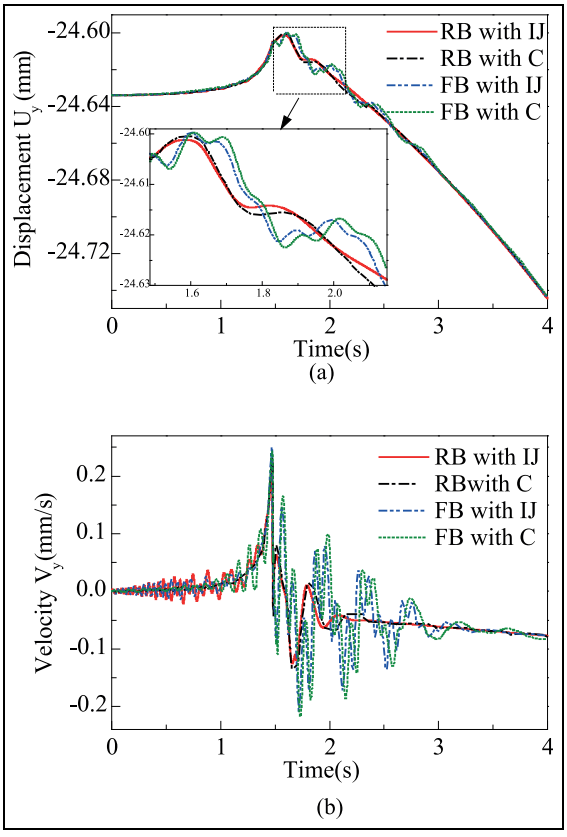

Figure 14. Displacement and velocity of main body of spacecraft: (a) displacement and (b) velocity.

in the deployment process, while the clearance and flexibility led to system vibration seriously at the initial operation stage and pre- and post-system lock stage.

Conclusion

Numerical simulations are conducted to reveal the effects of joint clearance and structural flexibility on the dynamic response of deployment of solar arrays system, which consists of main body, yoke, panels, torque spring mechanism, CCL mechanism, and lock mechanism. A contact model in joint clearance is established using the nonlinear Lankarani and Nikravesh model and the friction effect is considered using the amendatory Coulomb friction model.

The simulation results show that considering joint clearance and structure flexibility, the coupling between the structural elastic vibration and impact contact in clearance joint has significant effects on the dynamic characteristic of the deployable mechanism. Joint clearance generates impact force to disturb the deployment of solar arrays system, especially at initial operation stage and post-lock stage. Moreover, joint clearance generates friction force to delay the time for arrival of the expected lock position, while clearance can increase stability in deployment stage by adjusting the relative angle between pin and sleeve to reduce synchronous adjustment torques provided by CCL mechanism. Furthermore, the coupling of flexibility and clearance can be seen as a suspension system that may reduce the speed fluctuation in deployment stage, while the coupling of elastic vibration and impact in clearance joint further intensifies the jitter and instability of solar arrays system pre- and post-lock stage, which significantly affects the dynamic characteristic of the deployable system.

Besides, joint clearance and structure flexibility have significant effects on the satellite attitude with deployable mechanism. Therefore, in order to design effective controllers for eliminating the chaotic behaviors brought about by the non-linearity of joint with clearance and the complex couplings of vibration and shock of flexible body, the difference effects of clearance and flexibility on the dynamic characteristic of the deployable mechanism in different operation stage should be understood.

Downloaded from ade.sagepub.com by guest on September 29, 2016

The investigation supports the idea that the modeling of clearance and flexibility must be considered in analysis, design, and control of the deployable solar array system. Numerical simulations of deployment of solar arrays system under the gravity may be focused on in the future. Then, experimental research is necessary to verify the simulation analysis.

Declaration of conflicting interests

The author(s) declared no potential conflicts of interest with respect to the research, authorship, and/or publication of this article.

Funding

The author(s) received no financial support for the research, authorship, and/or publication of this article.

References

1. Puig L, Barton A and Rando N. A review on large deployable structures for astrophysics missions. *Acta Astronaut* 2010; 67: 12–26.
2. Li T, Guo J and Cao Y. Dynamic characteristics analysis of deployable space structures considering joint clearance. *Acta Astronaut* 2011; 68: 974–983.
3. Wallrapp O and Wiedemann S. Simulation of deployment of a flexible solar array. *Multibody Syst Dyn* 2002; 7: 101–125.
4. Kojima Y, Taniwaki S and Okami Y. Dynamic simulation of stick–slip motion of a flexible solar array. *Control Eng Pract* 2008; 16: 724–735.
5. Ge XS and Liu YZ. The attitude stability of a spacecraft with two flexible solar arrays in the gravitational field. Chaos. *Soliton Fract* 2008; 37: 108–112.
6. Gao E, Zhang X and Yao Z. Simulation and analysis of flexible solar panels' deployment and locking processes. *J Shanghai Jiaotong Univ* 2008; 13: 275–279.
7. Qi Z, Xu Y, Luo X, et al. Recursive formulations for multibody systems with frictional joints based on the interaction between bodies. *Multibody Syst Dyn* 2010; 24: 133–166.
8. Flores P, Leine R and Glocker C. Modeling and analysis of planar rigid multibody systems with translational clearance joints based on the non-smooth dynamics approach. *Multibody Syst Dyn* 2010; 2: 165–190.
9. Flores P. A parametric study on the dynamic response of planar multibody systems with multiple clearance joints. *Nonlinear Dynam* 2010; 61: 633–653.
10. Flores P, Ambrósio J, Claro JCP, et al. Lubricated revolute joints in rigid multibody systems. *Nonlinear Dynam* 2009; 56: 277–295.
11. Flores P, Ambrósio J, Claro JCP, et al. A study on dynamics of mechanical systems including joints with clearance and lubrication. *Mech Mach Theory* 2006; 41: 247–261.
12. Muvengei O, Kihiu J and Ikua B. Numerical study of parametric effects on the dynamic response of planar multi-body systems with differently located frictionless revolute clearance joints. *Mech Mach Theory* 2012; 53: 30–49.
13. Bai ZF, Liu YQ and Sun Y. Investigation on dynamic responses of dual-axis positioning mechanism for satellite antenna considering joint clearance. *J Mech Sci Technol* 2015; 29: 453–460.
14. Bai ZF and Zhao Y. Dynamics modeling and quantitative analysis of multibody systems including revolute clearance joint. *Precis Eng* 2012; 36: 554–567.
15. Li J, Yan S, Guo F, et al. Effects of damping, friction, gravity, and flexibility on the dynamic performance of a deployable mechanism with clearance. *Proc IMechE, Part C: J Mechanical Engineering Science* 2013; 227: 1791–1803.
16. Tian Q, Zhang Y, Chen L, et al. Simulation of planar flexible multibody systems with clearance and lubricated revolute joints. *Nonlinear Dynam* 2010; 60: 489–511.
17. Yan S and Guo P. Kinematic accuracy analysis of flexible mechanisms with uncertain link lengths and joint clearances. *Proc IMechE, Part C: J Mechanical Engineering Science* 2011; 225: 1973–1983.
18. Zheng E and Zhou X. Modeling and simulation of flexible slider-crank mechanism with clearance for a closed high speed press system. *Mech Mach Theory* 2014; 74: 10–30.
19. Khemili I and Romdhane L. Dynamic analysis of a flexible slider–crank mechanism with clearance. *Eur J Mech A: Solid* 2008; 27: 882–898.
20. Lankarani HM and Nikravesh PE. A contact force model with hysteresis damping for impact analysis of multibody systems. *J Mech Design* 1990; 112: 369–376.

Downloaded from ade.sagepub.com by guest on September 29, 2016